Biosensors and Bioelectronics 141 (2019) 111415

Contents lists available at ScienceDirect

Biosensors and Bioelectronics

journal homepage: www.elsevier.com/locate/bios

Multifunctional hand-held sensor using electronic components embedded in smartphones for quick PCR screening

Yoo Min Park, Chi Hyun Kim, Seok Jae Lee, Moon-Keun Lee*

Nano-bio Application Team, National NanoFab Center (NNFC), 291 Daehak-ro, Yuseong-gu, Daejeon, 34141, Republic of Korea

ARTICLE INFO

Keywords:
Smartphone-based biosensing platform
Point-of-care testing (POCT)
Pathogen optical biosensor
PCR screening

ABSTRACT

We focused on the development of a hand-held pathogen-detection device using smartphone-embedded electronic elements combined with functionalized magnetic particles (MPs) and sepharose. To perform affinity chromatography for evaluating DNA amplicons, avidin-conjugated MPs and succinimide-linked sepharose were used with biotin-primers. To mimic the centrifugal-based affinity ligand chromatography, a smartphone-mountable low-power fan was plugged into the charging port of a smartphone. The charging port stably emitted electric current at 3.0 V, and the fan blades were modified for use as a portable rotor. Based on the binding variation of MPs with DNA amplicons, the position of MPs in sepharose changed significantly during centrifugation. The change in distance was optically analyzed using the illumination sensor of the smartphone with respect to the altered transmittance due to the MPs. Amplified genes from *Escherichia. coli* O157:H7 samples ranging from 1.0×10^1 to 1.0×10^6 colony-forming units could be rapidly and immediately detected by the naked eye using a simple smartphone-based optical device. The results indicated that this novel biosensing technique is suitable for use as a point-of-care testing device in both industrial and clinical fields.

1. Introduction

The detection of pathogens in the food and other commercial industries is a major issue, since pathogenic microorganisms may lead to critical outbreaks of foodborne illnesses (Nyachuba, 2010; Arora et al., 2011; Mortari and Lorenzellim, 2014). To precisely identify pathogens, microbiological and biochemical evaluation techniques have conventionally been employed, such as culture and colony counting methods involving the counting of bacteria, or immunological analysis methods related to antigen–antibody interactions (DeBoer and Beumer, 1999; Iqbal et al., 2000; Gracias and McKillip, 2004; Skottrup et al., 2008). Although these methods are highly sensitive, inexpensive, and provide qualitative and quantitative information regarding target microorganisms, they are restricted by assay time or require initial enrichment of a target for accurate pathogen identification. Recently, polymerase chain reaction (PCR)-based molecular diagnostic techniques have been widely employed due to their high sensitivity for the detection of single copy of a target DNA sequence (Toze, 1999; Batt, 2007; Kim et al., 2007; Perry et al., 2007). In terms of specificity, sensitivity, rapidity, and accuracy for analyzing small amounts of target DNA, PCR methods demonstrate obvious merits in comparison with culture- or immunological-based detection techniques. In particular, fluorescence-based real-time polymerase chain reaction (RT-PCR) is employed as golden method in the clinical and medical field based on its high sensitivity and accuracy. However, despite these various advantages, PCR-based microbial detection is still restricted due to its high cost and complicated systems requiring skilled experts to perform the tests (Richards, 1999; Yang and Rothman, 2004; Smith and Osborn, 2009; Velusamy et al., 2010; Rahman et al., 2013). To fulfill the demand for PCR testing, various optical instruments, such as target-specific light sources, filters, prisms, and visualization devices have been developed. Nevertheless, the complexities of RT-PCR method necessitate a high cost and limitation in the target DNA detection to user (Toman, 2004; Almassian et al., 2013). Furthermore, these complex systems are limited when it comes to rapid screening of PCR products in the field.

To effectively minimize the conventional apparatus needed for use in the molecular diagnostic field as a point-of-care testing (POCT) devices, novel biosensing platforms have been widely studied, leading to improvements in devices and their availability by illuminating and minimizing biosensing components and systems (Park et al., 2015, 2017, 2018, 2019; Tiwari et al., 2015; Hwang et al., 2016; Kim et al., 2016; Yang et al., 2018). These platforms have been successfully evaluated for the pathogen detection employing the microfluidics, functionalized particles, or minimized devices with optical and electrochemical analysis method. Previous researchers have employed the

* Corresponding author.
E-mail address: mklee@nnfc.re.kr (M.-K. Lee).

https://doi.org/10.1016/j.bios.2019.111415
Received 3 April 2019; Received in revised form 24 May 2019; Accepted 4 June 2019
Available online 07 June 2019

various functionalities using detection principles such as affinity chromatography (Hwang et al., 2016), nano-particle functionalization (Park et al., 2015), capillary force-based fluidic assay (Kim et al., 2016), or carbon-family substrates (Tiwari et al., 2015) for sensitive evaluation of amplified gene. Although high-tech biosensing techniques and equipment allows for highly reliable molecular diagnosis (Uys et al., 2009), most have tried to scale-down bench-top level devices, such as fluorescence microscopy or electrochemical analysis systems, so that the developed POCT devices could be used at the laboratory facility level. These highly technical biosensors make them inaccessible to general patients and users (Mabey et al., 2004; Peeling and Mabey, 2010).

Many researchers have attempted to develop practical and useful POCT devices and systems for use in resource-limited settings, according to the World Health Organization (WHO) AS-SURED criteria (Affordable by those at risk of infection, Sensitive, Specific, User-friendly, Rapid and robust, no Equipment, Delivered to those who need it) (Drain et al., 2014). The simple detection principle is essential in order to overcome the critical issues around the simplification of complex biosensing systems and cost reduction (Tomazelli Coltro et al., 2014). In general, molecular analysis has conventionally employed fluorescence and colorimetric techniques related to target-specific optical instruments (Ahrberg et al., 2015; Morbioli et al., 2017; Huang et al., 2017; Kudr et al., 2017; Yin et al., 2017). However, these methods require complex methods with lab-scale instruments, and are inconvenient for detecting PCR products in the research and clinical fields.

To develop a practically useful POCT system, we designed a smartphone-based simple analysis system for PCR screening by utilizing the multifunctional built-in electronic components of smartphones. In our previous research, we successfully demonstrated the magnetic particle (MP)-based naked-eye detection principle, which has high sensitivity and reproducibility (Park et al., 2019). A colorimetric visualization with naked-eye detection for molecular diagnosis during POCT has considerable merit in terms of minimization of color development time, decreased washing procedures, and shorter reaction times, although this system still requires a bench-top-scale centrifuge. Thus, to successfully minimize the analytical methods and techniques, a centrifuge and optical analysis system were developed using a handheld smart IT device. In general, the electrical power output of a smart IT device can provide sustainable and stable low-power electricity via its charging port. By using these electrical properties low-power electronics, such as a smartphone-mountable fan, in conjunction with a three-dimensional (3D)-printed device, can be applied to create a portable centrifuge system. Additionally, the light sensor embedded in smart devices can rapidly detect ambient light, and light intensity can be displayed on-screen via an application. Therefore, the light sensor on a smart device was employed as a light detector with a 3D-printed holder. Based on this smart device-based biosensing platform, we wanted to verify its application for analyzing bacteria that cause foodborne illnesses; *Escherichia coli* O157:H7 (*E. coli* O157:H7) was selected as a biomarker. By employing our novel sensing system, we successfully simplified the PCR analysis platform by converting the conventional high power, gel electrophoresis, and UV-related detection needed into low battery power, visualized MPs, and an illumination sensor. The details of this test are reported here.

2. Materials and methods

2.1. Apparatus and materials

N-Hydroxysuccinimidyl Sepharose® 4 Fast Flow (H8280) was purchased from Sigma Aldrich (USA). Dynabeads® Myone™ Streptavidin C1 (65001) was purchased from Invitrogen (USA). HotStarTaq® Plus Master Mix kit (203643) was obtained from Qiagen (Germany). The primer was modified and synthesized by Bioneer (Korea). GelRed™ Nucleic Acid Gel stain 10,000X (41002) was purchased from Biotium (USA). A centrifuge (Combi-514R) was obtained from Hanil Scientific (Gimpo-si, Korea). Test tubes (AXY-MCT-060) were obtained from Axygen (USA). The UV exposure device (Slite 140) was purchased from AveGene (Taiwan). QuickExtract™ DNA extraction solution 1.0 (QE09050) was purchased from Epicentre (USA). The thermal cycler PCR System (C1000 Touch™, 184100) was purchased from Bio-Rad (USA). A tachometer (DT-2234B) was obtained from BlueBird (China). Smartphone-adaptable micro 5-pin-type portable fans (DMF-1004) were purchased from WiiX (China). The 3D-printed holder was fabricated using a Kings 3035 3D printer (Kings, China).

2.2. E. coli O157:H7 preparation in broth and milk

E. coli O157:H7 were cultured for 16 h at 37 °C in 10 mL Luria–Bertani (LB) medium with 1 g sodium chloride, 0.5 g yeast extract, and 1 g tryptone in 100 mL deionized (DI) water. To estimate the number of colony-forming units (CFU), colonies were counted using the colony counting method. Suspended *E. coli* O157:H7 samples were inoculated into broth and milk solutions, and the prepared pathogen cells were serially diluted to prepare various concentrations of target cells, from 1.0×10^1 to 1.0×10^6 CFU *E. coli* O157:H7 per 1 mL broth or milk. The prepared samples were stored at 4 °C until use. Prior to being inoculated into samples, the pathogen cells were harvested in test tubes by centrifugation at 13,000 rpm for 10 min, and bacterial DNA was extracted from the cell pellets using QuickExtract™ DNA solution 1.0 at 98 °C for 15 min.

2.3. PCR for E. coli O157:H7

E. coli O157:H7 genes at the various prepared concentrations in broth and milk were amplified using conventional thermal cycling PCR techniques. The primer were designed with stx2 DNA (Sharma et al., 1999). The 5′ end of the forward primer was conjugated with biotin to bind with streptavidin on the MPs. The forward primer sequence was 5′-GGGCAGTTATTTTGCTGTGGA-3′, while the reverse primer was 5′-TGTTGCCGTATTAACGAACCC-3′. PCR amplification was implemented using the HotStarTaq® Plus Master Mix Kit including 2X master mix, 0.08 μM each of forward and reverse primer, 1 μL extracted DNA, MgSO4, dNTP (dATP, dGTP, dCTP, and dTTP), and DI water. Thermal cycling PCR was performed under the following conditions: 5 min at 95 °C for pre-denaturation, 95 °C for 30 s for denaturation of double-stranded DNA templates, 60 °C for 30 s for annealing of primers, 72 °C for 30 s for synthesizing DNA, and 72 °C for 5 min for the final elongation step. The thermal cycle was repeated 35 times. The size of the biotin-conjugated target DNA was 120-bp amplicons.

2.4. Manipulation of the smart IT device-based low-power rotor module and its operation

The low-power rotor based on a smart IT device consisted of a 5-pin-type portable fan and the 3D-printed holder. The head of a portable fan was modified to join with the holder, as shown in Fig. 2(A) (*vide infra*). The 3D-printed test tube holder was joined with the portable fan head using a ring holder. The amplified PCR product evaluation was begun using the portable rotor module as follows: after performing PCR, the cocktail mixture, including 10 μL biotinylated amplicons, 10 μL MP (10 ng/mL), 10 μL, and 1 μL GelRed, was loaded into the sepharose-packed test tube; the test tube was then centrifuged using the portable rotor module by connecting it to a smartphone for 2 min.

2.5. Optical analysis using the illumination sensor on a smart IT device

The MPs that aggregated due to *E. coli* O157:H7 analysis were optically measured using the illumination sensor of a smart IT device. To construct an optical transduction system, we designed a smartphone-adaptable 3D-printed accessory consisting of a test tube holder, an LED

holder, and a smartphone holder. The white LED was directly connected to a 3 V external battery on the side wall of the accessory, and thus the LED could be turned on and off by connecting the LED wire to the battery. The 3D-printed accessory, which included the test tube containing precipitated MPs, was installed on the top of the smartphone to align the light source with the illumination sensor. The change in light intensity as it passed through the test tube was analyzed using the Lux Light Meter application (Doggo Apps, free version) on the Android operating system.

3. Results and discussion

3.1. Biosensing technique for amplified pathogen genes using a smart IT device

The biosensing technique developed here is based on a MP-based affinity chromatographic analysis that involves a chemical binding reaction between the mobile and stationary phases. The visualized metal particle family could be employed for the proposed sensing system, and MPs were selected for this study. The amine group of avidin on the MPs reacts strongly with N-Hydroxysuccinimide (NHS) on sepharose. The present reaction relied solely on the affinity between MPs and sepharose, while the amplicons conjugated with biotin could disturb this chemical coupling by steric hindrance of the specific reaction between biotin and avidin. Using the utilized smartphone-based centrifugal system, the MPs with PCR product was precipitated at the bottom of test tube by passing through the sepharose, while the MPs without PCR product was aggregated at the top of test tube. Based on these properties, the migration level of MPs in sepharose changed in accordance with the binding of amplicons during centrifugation (Fig. 1(A)). In a previous study, we successfully demonstrated these MP-based affinity principles. However, the previous system still required a bench-top scale centrifuge, so the smart IT device-based POCT system was developed to effectively minimize this complex system. In research conducted using IT devices up until now, the cameras on smartphones have been mainly employed to make use of a device's optical biosensing system. In order to improve the conventional system, we used a smartphone as a power supply via its charging port. This indicated that a portable fan was stable when operated at 3 V, making the novel portable centrifuge system possible (Fig. 1(A)). The 3D-printed accessory was connected to the portable fan to hold the test tubes. In accordance with the binding of pathogen amplicons, the precipitated MPs could be simply and rapidly detected by the smartphone's built-in optical detection function related to the illumination sensor.

In order to demonstrate the functionality of proposed sensing system, a feasibility test for the smartphone-based rotor module was established. Sepharose solution (200 μL) was added to the test tube, as shown in Fig. 1(B). Next, MPs with 1.0×10^5 CFU *E. coli* O157:H7 amplified genes were loaded into the sepharose. The prepared test tube was inserted into the 3D-printed holder, and another test tube containing the same volume was simultaneously inserted into the opposite side to maintain the balance of the centrifugal force. Any smart IT device with a micro-5-pin port, such as a smartphone, a tablet, or an external battery, could act as a power supply. In this study, an LG G4 (F500) smartphone was employed. As shown in Fig. 1(B), the rotor module was operated by connecting it to the smartphone, allowing stable rotation of the test tube. The MPs should gradually migrate over time. As a result, the migration of MPs clearly changed as they reacted with the amplicons. Test tubes containing precipitated MPs were sequentially analyzed using the illumination sensor-based optical analysis

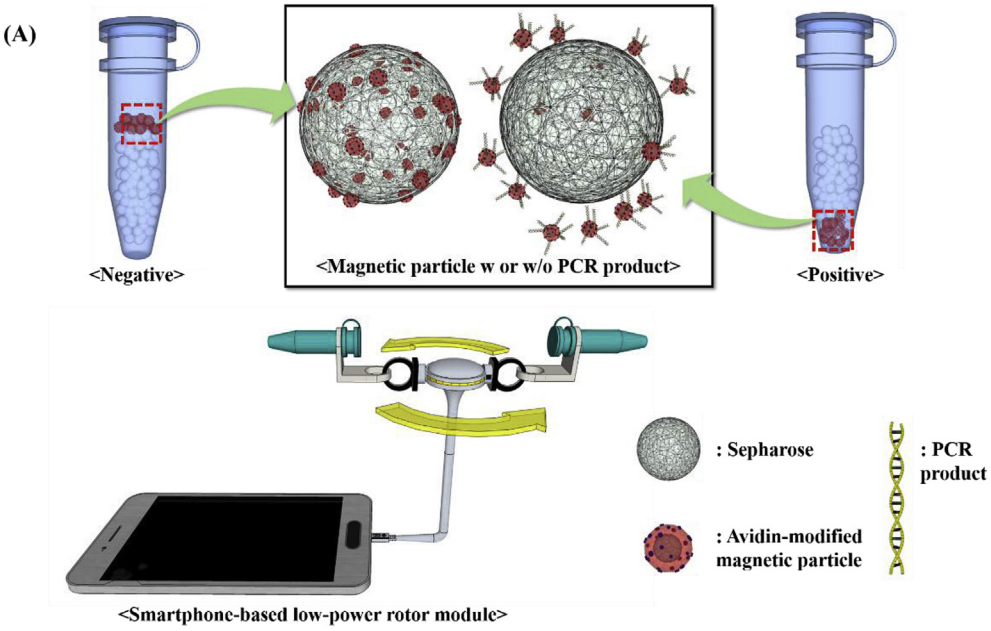

Fig. 1. Schematic diagram of the smart IT device-based low-power rotor module for pathogenic strain assessment. (A) Magnetic particles (MPs) were employed as the mobile phase and sepharose as the stationary phase. The avidin-modified MPs chemically reacted with N-Hydroxysuccinimide (NHS)-sepharose. In order to create a minimized centrifugal system, a portable fan was used as a rotor module, which was then operated by a smart IT device. (B) The smart IT device-based test procedure. MPs with amplified genes of *E. coli* O157:H7 were loaded into sepharose-packed test tubes. The test tubes were centrifuged using the portable rotor module for 2 min. MPs that reacted with amplicons aggregated at the bottom of the tube, while pristine MPs remained at the top of the sepharose.

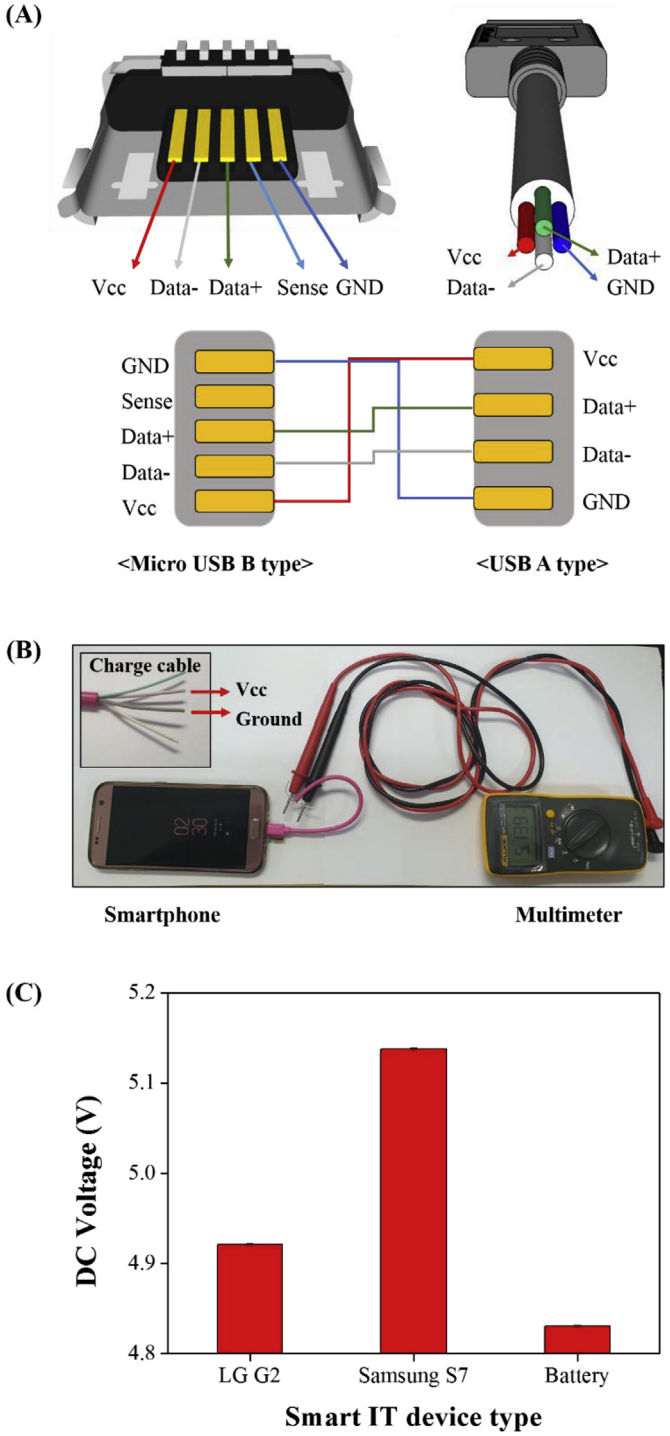

Fig. 2. Construction of the power unit using a portable USB cable and testing for output voltage of different types of smart IT devices. (A) An illustration of micro USB B and USB A type cable compositions and connectivity. Vcc, $Data^{-}$, $Data^{+}$, and GND were common to both. (B) Voltage measurement of smart IT device outputs using a multimeter with a modified cable wire. (C) Voltage test results for (B). Each test was conducted three times; error bars indicate standard deviations.

system, and the quantification in accordance with the concentration of *E. coli* O157:H7 tested was immediately evaluated by the application. Based on the proposed technique, amplified pathogen genes were rapidly evaluated by employing a smart IT device and a simple method.

3.2. Use of the low-power electricity supply embedded in smart IT devices

The voltage of power inputs and outputs in smart IT devices varies with manufacturing specifications. Therefore, the output voltage of diverse smart IT devices should be confirmed for use with the low-power rotor module. In general, smart IT devices contain a micro USB B-type port with five pins, while portable low-power devices have a USB A-type port with four pins. Both USB type have four pins in common, including the ground (GND), a voltage common collector (Vcc), Data +, and Data −, while the USB B-type additionally has a Sense pin (Fig. 2(A)). Of these pins, the GND and Vcc pins are involved with the power supply, while the Data + and Data − pins are related to bidirectional data transmission. The Sense pin works for the specific response of own smart IT devices. Therefore, portable electronic devices usually operate using the GND and Vcc pins. In order to accurately confirm the capability of the electrical power output, the voltage of the smart IT device was measured using a multimeter (Fig. 2(B)). The electrical power of the smartphone was exploited by connecting a USB A cable that was modified to expose the GND and Vcc wires. Three types of smart IT devices, an LG G2, a Samsung Galaxy S7, and an external battery were tested, and the output voltage of each device was repeatedly measured by eliminating any residual electricity. The output voltages were 4.9, 5.1, and 4.8 V for the LG G2, Samsung Galaxy S7, and external battery, respectively (Fig. 2(C)). In order to accurately evaluate the stability of the output voltage, the tests were repeated at least three times under same condition, and the results are presented in Fig. 2(C) with error bar. The obtained standard deviation (SD) of the output voltages were less than 0.01%, indicating high stability of electric supply. The variation in output voltage is that they each have their own characteristics, according to the device model or manufacturer. Considering that the operating voltage of commercial low-power devices is approximately 3–3.5 V, all smart IT devices are potentially useful. Here the Samsung Galaxy S7 was selected for the following tests owing to its relatively high voltage power and stability. The test results obtained demonstrate the possibility for the manipulation of low-power devices for various applications.

3.3. Feasibility testing of the smartphone-based low-power centrifuge system

To observe separated MPs following their reaction with the PCR product, a certain physical force is required for the MP migration. To successfully establish the simplification of a rotational device to enable the practical use of a POCT device as a diagnostic tool for pathogens, we designed and fabricated a portable rotor. A schematic diagram of this battery-powered portable rotor is shown in Fig. 3(A). The fabricated rotor consisted of a power connector, a scaffold, a motor, and a holder. A mini-fan that could be operated via a micro-5-pin-type port was used. The selected fan performed well at 3–3.5 V direct current (DC) voltage. Thus, low-power sources, such as a smartphone or an external battery are suitable, as we previously revealed. The fan blades were removed so that the test tube holder, which was fabricated using a 3D-printing method, could be installed. The fabricated holder included a test tube holder and a ring linker to connect to the motor head.

In this study, the efficiency of MPs migration in the test tube was directly related to the velocity of the low-power fan. Therefore, by using the rotor, the revolutions per minute (RPM) of the fan could be tested to verify the performance of the embedded motor. The weight of the test tube; volumes of 0–600 μL DI water were used to provide a variety of weights. Adhesive silver-foil tape was attached to the side wall of the test tubes, and a tachometer was used to measure rotational speeds (RPM), as shown in Fig. 3(B). The result of test was recorded, and the data are presented in Fig. 3(C). A steady rotational velocity of 2000 RPM was recorded in the test using an empty tube. Then, the prepared DI water samples were sequentially tested. In the 200 μL DI water test, a velocity of approximately 1900 RPM was observed, and this velocity was also obtained with 400 μL DI water. The fan velocity

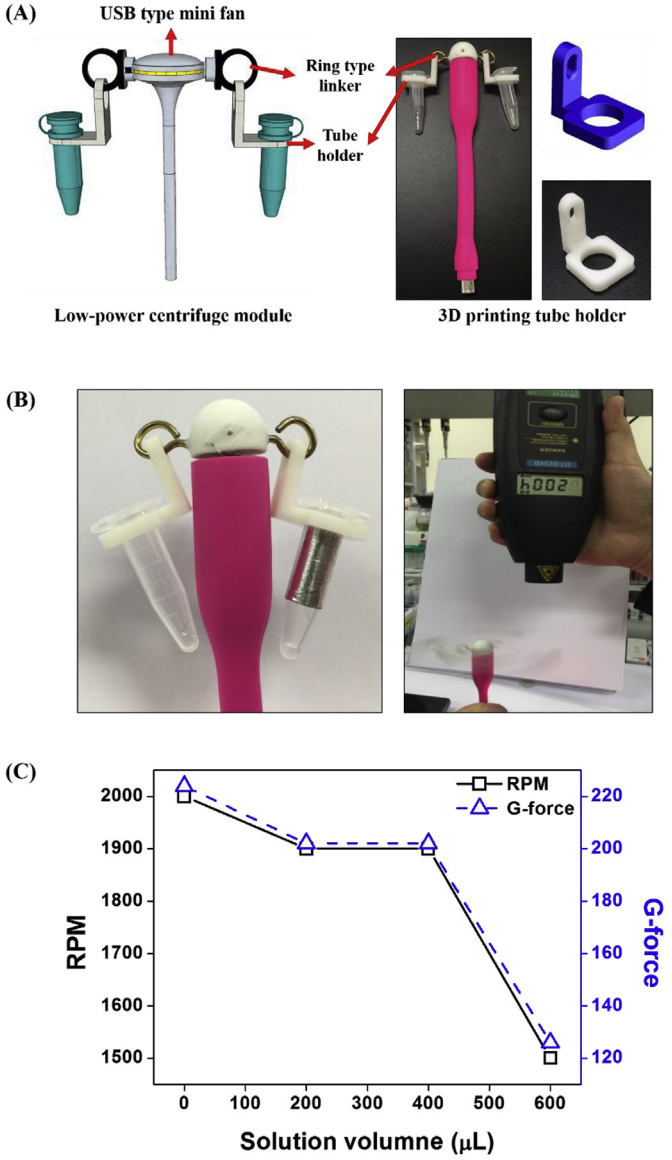

Fig. 3. (A) Construction of the portable rotor module. A portable USB-type fan was employed as a minimized low-power motor. A 3D-printed accessory was produced to hold the test tube. (B) The velocity of the test tube spinning in the portable rotor was measured using a tachometer. (C) The velocities of test tubes containing DI water of volumes 200, 400, and 600 μL were recorded.

decreased when volumes of more than 600 μL were tested, indicating that the rotor power of the motor operated properly only with volumes of less than 400 μL. The velocity slowly decreased with increasing volumes of solution, as expected. Based on the test results, the gravitational force (g-force) for each test was calculated using the following equation:

$$g = (1.118 \times 10^{-5}) R (RPM/1000)^2$$

where g is the g-force and R is the radius of gyration (cm). The calculated g-force is also shown in Fig. 3(C). A force of 220 g was achieved using the empty tube test, while approximately 200 g was achieved in the 200–400 μL DI water tests. The g-force decreased with volumes of more than 600 μL. Based on these test results, a sample volume of 400 μL was determined to be ideal for separation of MPs.

3.4. Evaluation of *E. coli* O157:H7 using the novel sensing technique

Based on the newly established and optimized biosensing platform, *E. coli* O157:H7 genes from cultures containing 1.0×10^1 to 1.0×10^6 CFU were evaluated. The prepared *E. coli* O157:H7 was extracted and purified, and genes were amplified using a conventional PCR technique. DI water was used as a negative control. Prior to concentrating the prepared *E. coli* O157:H7 sample using the rotor module, amplified genes were firstly verified using gel electrophoresis, and the resulting image is shown in Fig. 4(A). The designed target gene size was 120 bp, and a PCR band from the whole gene was clearly present at the related PCR marker band. In addition, band intensity gradually increased with increasing concentration of the target *E. coli* O157:H7 gene, while the band was not detected in the negative control, indicating that the target gene was accurately prepared. The remaining target gene samples were applied using the newly developed biosensing system under the same conditions as the previous test. To verify reproducibility, the intra- and inter-assays were performed under the same conditions each time, such as reaction time, pH, and humidity. Representative images of the results are shown in Fig. 4(A). MPs clearly migrated to the bottom of the test tubes containing the *E. coli* O157:H7 target genes, while changes in the level of MPs were not detected in the negative control. In the tube containing the 1.0×10^1 CFU sample, the MPs moved only slightly related to the 1.0×10^2 to 1.0×10^6 CFU *E. coli* O157:H7 samples, the assumption being that the amplified gene was insufficient to fully aggregate the particle surfaces. However, the 1.0×10^1 CFU differed significantly from the negative control, and thus we concluded that the limit of detection (LOD) from repeated test results using the newly developed sensing platform was 1.0×10^1 CFU *E. coli* O157:H7.

To verify the practical applicability of this approach, an analysis was performed using real samples. Artificially infected real food samples were prepared by inoculating 10 μL milk with 1.0×10^6 CFU *E. coli* O157:H7, adding stock solution that had been serially diluted 10-fold into milk. Then, the *E. coli* O157:H7-inoculated milk samples were lysed and purified, and the prepared sample was analyzed using a conventional PCR device. PCR bands were clearly shown (Fig. 4(B)), indicating that the sample was accurately prepared. The same sample was then analyzed using the newly developed rotor module. The tests were performed repeatedly, under the same conditions, including pH, temperature, and reaction time, and representative test results are shown in Fig. 4(B). The migration of MPs was clearly observed in the positive test sample, while no movement of MPs was detected in the negative control, indicating the high sensitivity of the manufactured biosensing platform for real sample-based *E. coli* O157:H7 evaluation. The results revealed that the smartphone-based low-power rotor could provide sufficient centrifugal force to analyze *E. coli* O157:H7 in real milk samples, and that 1.0×10^1 CFU *E. coli* O157:H7 was sensitively evaluated in broth and milk, demonstrating the high sensitivity with LOD of 1.0×10^1 CFU. Based on these findings, the battery-powered portable rotor we developed for the analysis of PCR products could be employed as an on-site inspection tool, as we successfully established that it is a reliable molecular sensing platform based on significant test results showing high reproducibility and sensitivity.

3.5. Use of the smart IT device-based optical biosensing platform

In order to clearly detect the migration levels of MPs, we introduced a smart IT device-based optical analysis system. In a previous study, a POCT optical device was successfully established by using the illumination sensor on a smart IT device, which can sensitively and rapidly measure light intensity. Using these principles, aggregated MPs could be rapidly measured. The proposed sensing system consists of a light source, a test tube, and an illumination sensor on a smart IT device (Fig. 5(A)). The intensity of light passing through the bottom of the test tube changes for *E. coli* O157:H7-positive samples, but is unchanged in the negative test. The altered light intensity can be rapidly analyzed by the illumination sensor and associated software embedded in the smartphone, and the light level is numerically displayed on screen. The

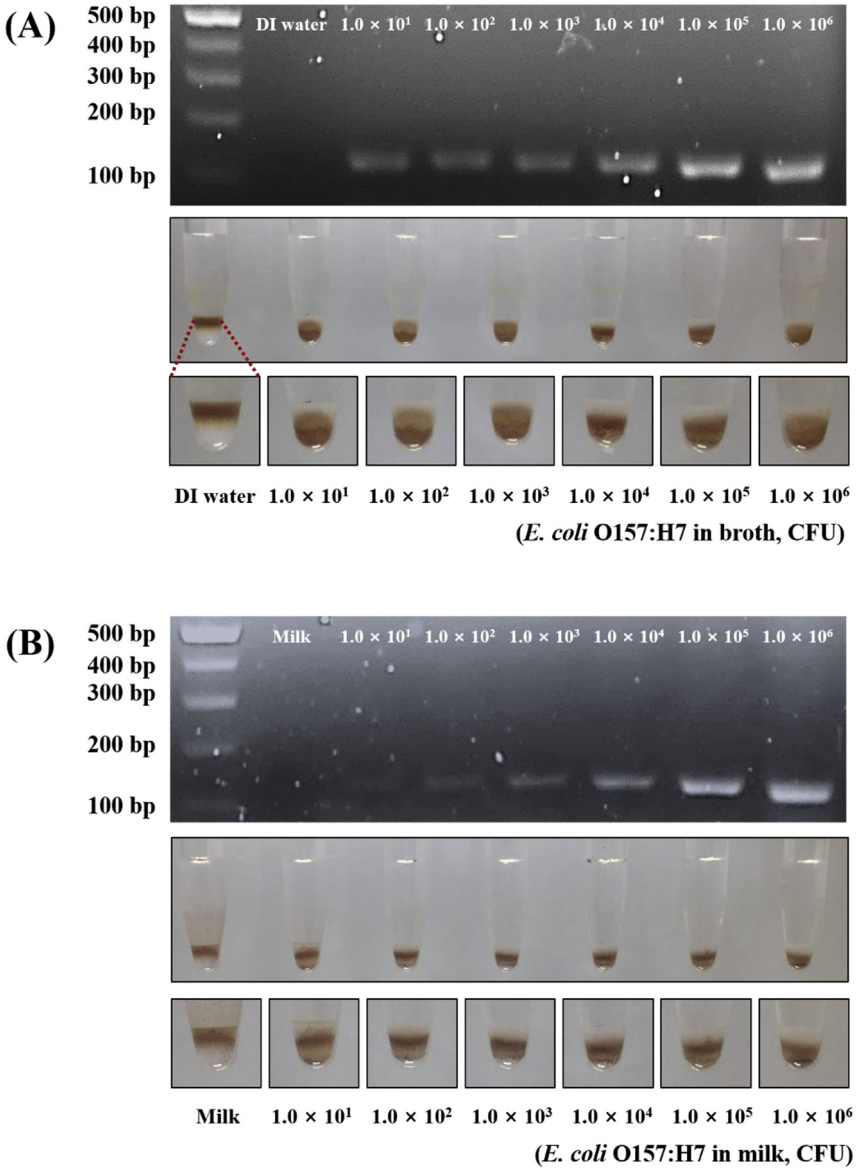

Fig. 4. (A) A gel electrophoresis image for prepared *E. coli* O157:H7 in the concentration range from 1.0×10^1 to 1.0×10^6 CFU cultured in Luria–Bertani (LB) broth, and the test result for MP-based *E. coli* O157:H7 evaluation using the fabricated portable rotor module. (B) Test results of *E. coli* O157:H7 in a real milk sample using the same method as (A).

sensing principle was based on transmittance levels according to the amount of MPs and sepharose. To analyze absorbance, 200 μL of each material was loaded onto a 96-well plate, and the optical density of each well was measured. As shown in Fig. 5(B), the maximum absorbance of MPs was about 2.5 A.U. at 500 nm, while the optical density in the whole detection range, from 400 to 1000 nm, was more than 2 A.U. However, the absorbance of sepharose was less than 0.5 A.U. in the same detection range. These results reveal that aggregated MPs in sepharose could be accurately detected by the optical-based sensing system. Based on these results, MPs and sepharose were sequentially tested using the illumination sensor on the smartphone. Owing to the difference in optical intensities in the whole detection range, including visible and infrared, a white LED was employed as the light source, and the test was implemented in dark conditions to avoid interference with ambient light. The MPs and sepharose (100 μL) were then loaded into a transparent polydimethylsiloxane (PDMS) chip, and the chip was placed over the illumination sensor on the smartphone, as shown in Fig. 5(C). The white LED light that passing through the PDMS was analyzed using the LuxMeter application. In the test, lux values of 308 and 1025 were recorded for MPs and sepharose, respectively; these results were repeatedly and uniformly obtained under the same conditions. Taken together, these results indicated that MPs and sepharose can be accurately analyzed using the smart IT device-based optical sensing system.

3.6. *E. coli O157:H7 evaluation using smart IT device*

Based on the reliability and feasibility of the previous result, we successfully demonstrated a smartphone-based optical transduction system. A 3D-printed device, including a test tube holder, smartphone holder, and light source holder, was designed and fabricated, as shown in Fig. 6(A). A white LED was installed in front of the test tube, and a 3 V external battery was fixed to the side of the 3D-printed device, in conjunction with the LED. The fabricated 3D-printed accessory was installed at the top of the smartphone, and the optical density of an empty test tube was found to be 1570 lux. Then, MPs with *E. coli* O157:H7 samples which were centrifuged using the smartphone-based rotation module were sequentially tested. *E. coli* O157:H7 from the

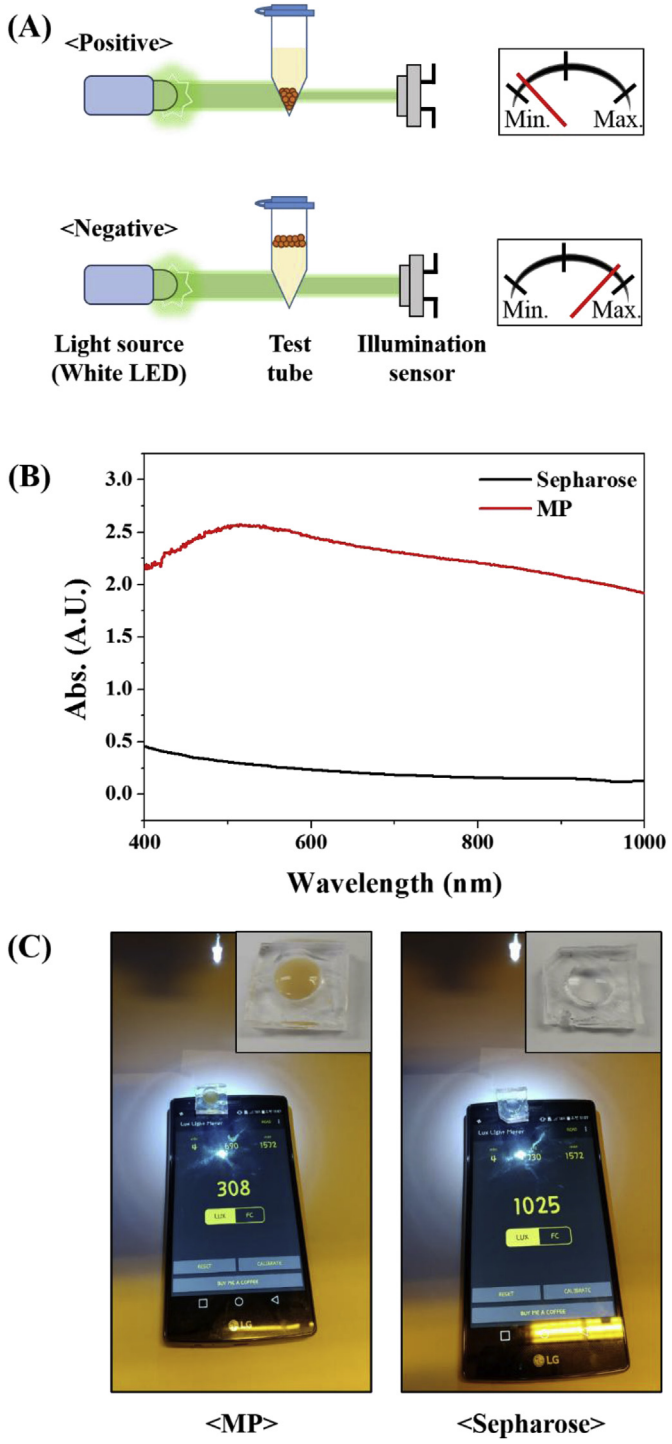

Fig. 5. The illumination sensor-based optical analysis technique and absorbance test using MP and sepharose. (A) Changes in light intensity passing though magnetic particles (MPs) or sepharose. (B) Absorbance evaluation of both MPs and sepharose. (C) The optical transmittance test of MPs and sepharose in the PDMS chamber, using the illumination sensor on the smartphone. The test was carried out in dark conditions, and an external white LED was employed and used at a fixed distance.

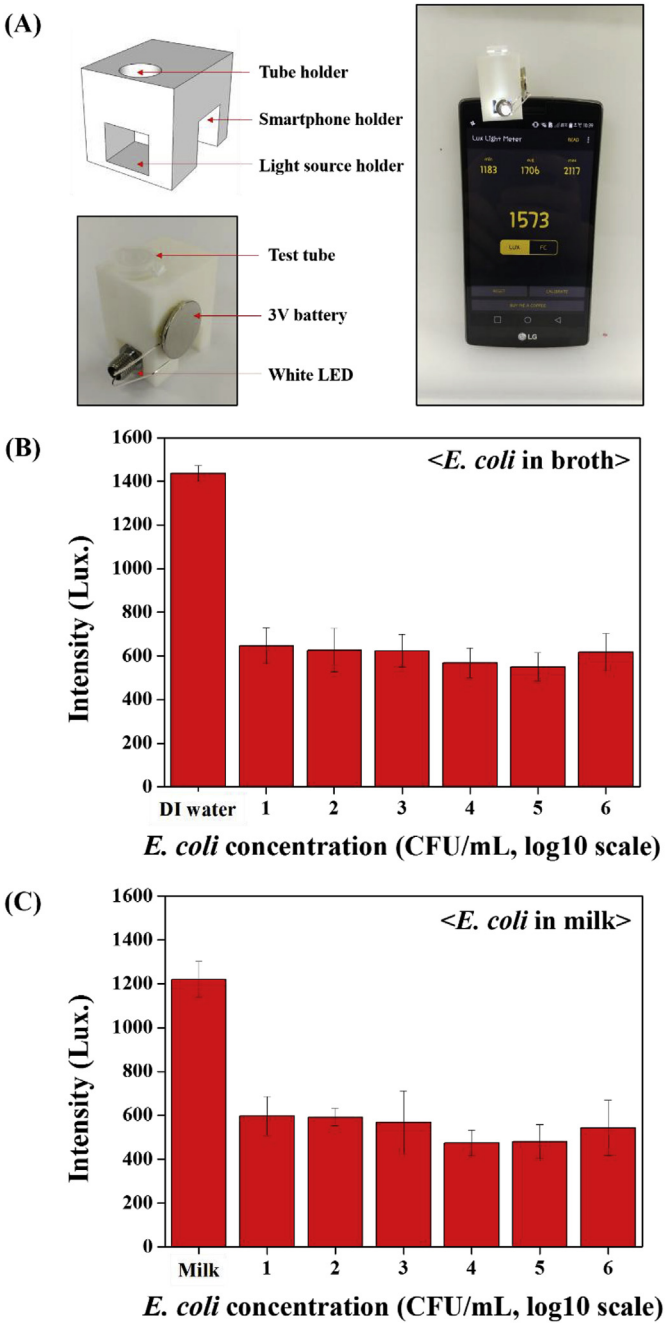

Fig. 6. (A) The 3D-printed accessory for the smartphone-based optical sensing platform. The accessory contains holders for a test tube, white LED, 3 V battery, and smartphone. (B) Optical signals for MP-based *E. coli* O157:H7 testing using an illumination sensor. Samples of 1.0×10^1 to 1.0×10^6 CFU *E. coli* O157:H7 cultured in broth were analyzed. (C) Test results of *E. coli* O157:H7 in real milk samples under the same conditions as (B). The same test was repeated three times under the same conditions; error bars show standard deviations.

broth sample was loaded first, and the results are shown in Fig. 6(B). For the DI water test, about 1400 lux was recorded, while approximately 600 lux was recorded for the applied detection range from 1.0×10^1 to 1.0×10^6 CFU/mL samples of *E. coli* O157:H7. Although the average values of the optical signal from each test result were slightly different, the lux value across the whole detection range was less than 800 lux, indicating that 800 lux could be used as a cut-off value to determine the existence of pathogens. Based on these results, the LOD was 1.0×10^1 CFU/mL *E. coli* O157:H7. To evaluate repeatability, the same test was repeatedly implemented at least three times under the same conditions of pH, temperature, and reaction time. The SD is presented in Fig. 6(B) as an error bar, and was 11% for the whole detection range. Based on these values, the sensing system demonstrated high sensitivity and reproducibility when testing for *E. coli* O157:H7.

To verify the system's practical application, real samples were also

tested. Milk samples inoculated with 1.0×10^1 to 1.0×10^6 CFU/mL *E. coli* O157:H7 were analyzed using the fabricated smartphone sensor. As shown in Fig. 6(C), the optical signal of the milk test was observed to be about 1200 lux, while the average optical intensity from the range of *E. coli* O157:H7 samples was between 500 and 600 lux. The obtained signals were relatively lower than those of the broth test, due to the interference of various proteins in milk, such as albumin, casein, and enzymes. Although milk contains these various components, the affinity chemical-based MPs reaction technique preferentially binds with target pathogens, and also migrates into sepharose sufficiently to be detected. In order to verify the repeatability for intra- and inter-signal variation, the same tests were repeated three times under the same conditions such as pH, temperature, and reaction time. The calculated SD for the whole detection range was 14%, demonstrating the high repeatability of the biosensing platform for real sample-based pathogen determination. The test results showed that the lux value of *E. coli* O157:H7 concentrations ranging from 1.0×10^1 to 1.0×10^6 CFU/mL was clearly distinguishable from the negative control, and thus we concluded that the LOD when testing real samples was 1.0×10^1 CFU/mL *E. coli* O157:H7. Based on the obtained results, we concluded that the utilized low-power rotor could clearly analyze the whole detection range of applied *E. coli* O157:H7 gene both in broth and real milk samples, and the 1.0×10^1 CFU *E. coli* O157:H7 was accurately determined, indicating the high sensitivity of developed smartphone-based biosensing platform (LOD with 1.0×10^1 CFU). The price for single assay considering the consumable materials such as magnetic particle, sepharose, PCR mixture, and test tube was about $5 USD, making this assay highly accessible to various user.

The smartphone-based biosensing system enables commonly used methodologies on a portable apparatus for quick on-site PCR screening, and thus the developed sensing platform was shown to be suitable for analyzing the diverse pathogen gene amplified by conventional PCR method even in the food. We believe that this device makes a significant contribution to the principle of simplifying analysis of pathogens that cause foodborne illnesses POCT device.

4. Conclusion

Here, MP-based pathogen amplicon quantification technique involving a centrifugal system was effectively performed using a low-power electronic smart IT device. Based on colorimetric chromatography of the MPs using simple chemical affinity, the amplified PCR product was easily visualized and evaluated using a portable electronic device. The fabricated biosensing system successfully reduced both costs and test times (to as little as 3 min) for the accurate verification of a pathogenic strain of *E. coli* O157:H7 in real food samples. The smart IT device-based optical sensing system also demonstrated high reproducibility (10%) for pathogen genes in samples in the concentration range of 1.0×10^1 to 1.0×10^6 CFU, with high sensitivity and a LOD of 1.0×10^1 CFU. This minimized biosensor system, based on the multifunctionalities of smart IT devices, provides an advanced analysis tool in the commercial field owing to the high applicability of low-power electronic devices in various biosensor approaches, such as quick PCR screening. The reliability of the findings in this study exhibit significance for the development of portable optical biosensing techniques for POCT devices as useful tools for pathogen assessment.

CRediT authorship contribution statement

Yoo Min Park: Writing - original draft, Methodology, Investigation, Data curation. **Chi Hyun Kim:** Validation, Formal analysis, Investigation. **Seok Jae Lee:** Funding acquisition, Project administration. **Moon-Keun Lee:** Validation, Writing - review and editing, Supervision.

Acknowledgments

This work was supported by Nano Material Technology Development Program through the National Research Foundation (NRF) of Korea funded by the Ministry of Science and ICT (MSIT) (No.2017M3A7B4039936), and Medical Research Center Program through the NRF of Korea funded by MSIT (No. 2014R1A5A2010008). Also, this work was supported by the BioNano Health-Guard Research Center funded by the MSIT of Korea as Global Frontier Project (Grant number H-GUARD_ 2014M3A6B2060302).

References

Ahrberg, C.D., Manz, A., Neuzil, P., 2015. Sci. Rep. 5 11479.
Almassian, D.R., Cockrell, L.M., Nelson, W.M., 2013. Chem. Soc. Rev. 42, 8769–8798.
Arora, P., Sindhu, A., Dilbaghi, N., Chaudhury, A., 2011. Biosens. Bioelectron. 28, 1–12.
Batt, C.A., 2007. Science 316, 1579–1580.
DeBoer, E., Beumer, R.R., 1999. Int. J. Food Microbiol. 50, 119–130.
Drain, P.K., Hyle, E.P., Noubary, F., Freedberg, K.A., Wilson, D., Bishai, W.R., Rodriguez, W., Bassett, I.V., 2014. Lancet Infect. Dis. 14, 239–249.
Gracias, K.S., McKillip, J.L., 2004. Can. J. Microbiol. 50, 883–890.
Huang, J., Li, X.-Y., Du, Y.-C., Zhang, L.-N., Liu, K.-K., Zhu, L.-N., Kong, D.-M., 2017. Biosens. Bioelectron. 91, 417–423.
Hwang, S.-H., Kim, D.-E., Im, J.-H., Kang, S.-J., Lee, D.-H., Son, S.J., 2016. Biosens. Bioelectron. 79, 829–834.
Iqbal, S.S., Mayo, M.W., Bruno, J.G., Bronk, B.V., Batt, C.A., Chambers, J.P., 2000. Biosens. Bioelectron. 15, 549–578.
Kim, J.S., Lee, G.G., Park, J.S., Jung, Y.H., Kwak, H.S., Kim, S.B., Nam, Y.S., Kwon, S.-T., 2007. J. Food Prot. 70, 1656–1662.
Kim, Y.T., Lee, D., Heo, H.Y., Sim, J.E., Woo, K.M., Im, S.G., Seo, T.S., 2016. Biosens. Bioelectron. 78, 489–496.
Kudr, J., Richtera, L., Xhaxhiu, K., Hynek, D., Heger, Z., Zitka, O., Adam, V., 2017. Biosens. Bioelectron. 92, 133–139.
Mabey, D., Peeling, R.W., Ustianowski, A., Perkins, M.D., 2004. Nat. Rev. Microbiol. 2, 231–240.
Morbioli, G.G., Mazzu-Nascimento, T., Stockton, A.M., Carrilho, E., 2017. Anal. Chim. Acta 970, 1–22.
Mortari, A., Lorenzellim, L., 2014. Biosens. Bioelectron. 60, 8–21.
Nyachuba, D.G., 2010. Nutr. Rev. 68, 257–269.
Park, Y.M., Han, Y.D., Chun, H.J., Yoon, H.C., 2017. Biosens. Bioelectron. 93, 205–211.
Park, Y.M., Kim, C.H., Song, Y., Hwang, S.-H., Lee, S.J., Lee, M.-K., 2019. Talanta 195, 97–102.
Park, Y.M., Kim, S.J., Lee, K.J., Yang, S.S., Min, B.-H., Yoon, H.C., 2015. Biosens. Bioelectron. 67, 192–199.
Park, Y.M., Lim, S.Y., Shin, S.J., Kim, C.H., Jeong, S.W., Shin, S.Y., Bae, N.H., Lee, S.J., Na, J., Jung, G.Y., Lee, T.J., 2018. Anal. Chim. Acta 1027, 57–66.
Peeling, R., Mabey, D., 2010. Clin. Microbiol. Infect. 16, 1062–1069.
Perry, L., Heard, P., Kane, M., Kim, H., Savikhin, S., Dominguez, W., Applegate, B., 2007. J. Rapid Methods Autom. Microbiol. 15, 176–198.
Rahman, M.T., Uddin, M.S., Sultana, R., Moue, A., Setu, M., 2013. AKMMC J 4, 30–36.
Richards, G.P., 1999. J. Food Prot. 62, 691–697.
Sharma, V., Dean-Nystrom, E., Casey, T., 1999. Mol. Cell. Probes 13, 291–302.
Skottrup, P.D., Nicolaisen, M., Justesen, A.F., 2008. Biosens. Bioelectron. 24, 339–348.
Smith, C.J., Osborn, A.M., 2009. FEMS Microbiol. Ecol. 67, 6–20.
Tiwari, I., Singh, M., Pandey, C.M., Sumana, G., 2015. Sens. Actuators, B 206, 276–283.
Toman, K., 2004. What are the advantages and disadvantages of fluorescence microscopy? In: Tattersfield, A. (Ed.), Toman's Tuberculosis: Case Detection, Treatment, and Monitoring: Questions and Answers, second ed. World Health Organization, Geneva, pp. 31–34.
Tomazelli Coltro, W.K., Cheng, C.M., Carrilho, E., Jesus, D.P., 2014. Electrophoresis 35, 2309–2324.
Toze, S., 1999. Water Res. 33, 3545–3556.
Uys, P.W., Warren, R., van Helden, P.D., Murray, M., Victor, T.C., 2009. J. Clin. Microbiol. 47, 1484–1490.
Velusamy, V., Arshak, K., Korostynska, O., Oliwa, K., Adley, C., 2010. Biotechnol. Adv. 28, 232–254.
Yang, R.-J., Fub, L.-M., Hou, H.-H., 2018. Sens. Actuators, B 266, 26–45.
Yang, S., Rothman, R.E., 2004. Lancet Infect. Dis. 4, 337–348.
Yin, H.-S., Li, B.-C., Zhou, Y.-L., Wang, H.-Y., Wang, M.-H., Ai, S.-Y., 2017. Biosens. Bioelectron. 96, 106–112.